Computational and Structural Biotechnology Journal 19 (2021) 6000–6008

COMPUTATIONAL AND STRUCTURAL BIOTECHNOLOGY JOURNAL

journal homepage: www.elsevier.com/locate/csbj

Microbial interaction-driven community differences as revealed by network analysis

Zhe Pan [a], Yanhong Chen [a], Mi Zhou [a], Tim A. McAllister [b], Le Luo Guan [a,*]

[a] Department of Agricultural, Food and Nutritional Science, University of Alberta, Edmonton, AB, Canada
[b] Agriculture and Agri-Food Canada, Lethbridge Research Centre, Lethbridge, AB, Canada

ARTICLE INFO

Article history:
Received 15 July 2021
Received in revised form 23 October 2021
Accepted 28 October 2021
Available online 1 November 2021

Keywords:
Shiga toxin
Microbial interactions
Co-occurrence network
Group-specific taxa

ABSTRACT

Diversity and compositional analysis are the most common approaches in deciphering microbial community differences. However, these approaches neglect microbial structural differences driven by microbial interactions. In this study, the microbiota data were generated from 12 rectal digesta samples collected from steers in which the Shiga toxin 2 gene (*stx2*) was not expressed (defined as Stx2− group) in the bacteria, and those with *stx2* expressed (defined as Stx2+ group) and used to explore whether microbial networks affect gut microbiota and foodborne pathogen virulence in cattle. Although the Shannon and Chao1 indices of rectal digesta microbial communities did not differ between the two groups ($P > 0.05$), 24 and 13 taxa were identified to be group-specific genera for Stx2− and Stx2+ microbial communities, respectively. The network analysis indicated 12 and 14 generalists (microbes that were densely connected with other taxa) in microbial communities for Stx2− and Stx2+ groups, and 8 out of 12 generalists and 6 out of 14 generalists were designated to Stx2− and Stx2+ group-specific genera, respectively. However, the 66 core genera were not classified as network generalists. Natural connectivity measurements revealed that the higher stability of the Stx2− microbial network in comparison to the Stx2+ network, suggesting that the structure of each microbial community was inherently different even when their diversity and composition were comparable. Group-specific genera intensely interacted with other taxa in the co-occurrence network, indicating that characterizing microbial networks together with group-specific genera could be an alternative approach to identify variation in microbial communities.

1. Introduction

Assessing microbial profiles using diversity, composition, and abundance measurements are broadly adopted approaches that have been widely applied to determine the role of the microbiome in host health. For example, the lower richness of human fecal microbiota is associated with dyslipidemia and insulin resistance leading to obesity [1], and higher evenness of milk/teat microbiota is associated with dairy cow mastitis [2]. In addition to these quantitative measures, microbial taxa interact within ecological niches, forming "micro-communities" that may function collectively [3]. Such microbial interactions can be influenced by the host, which in turn affect the host's physiological activities. Hence, microbial interactions, together with microbial-host interactions, are critical for the establishment, maintenance, and function of microbiota [4].

The traditional and commonly used approach to identify microbial interactions is the construction of microbial co-occurrence networks using a correlation-based method (Pearson's or Spearman's correlation coefficient) [2,3,5,6]. This method is prone to detecting spurious correlations among low abundance taxa [7] and can lead to an ill-defined understanding of microbial interactions. These conventional methods also adopt subjective thresholds to define significant microbial interactions largely based on known biological information, while appropriate thresholds are hard to select, particularly for less studied and low abundant microorganisms [4,8]. Hence, effective ways to construct microbial co-occurrence networks are needed to enable an in-depth understanding of structural differences in microbial communities and how these could affect host-microbial interactions.

Shiga toxin-producing *Escherichia coli* (STEC) cause foodborne diseases that can lead to severe human infections (*i.e.* bloody diarrhea, hemolytic uremic syndrome) [9]. Cattle are the main asymptomatic carriers of STEC with the rectal-anal junction (RAJ) being the main colonization site [10]. As the result, cattle can shed STEC

* Corresponding author.
E-mail address: lguan@ualberta.ca (L.L. Guan).

https://doi.org/10.1016/j.csbj.2021.10.035

to the ambient environment and therefore promote cattle-cattle/human transmission [11,12]. Our recent research has reported that host (*i.e.* host genes, immunity, microRNAs [13–16])-microbial interactions may play a role in affecting STEC colonization in cattle. In addition, Shiga toxins (*stx*) are major virulence factors in STEC with prototype toxins being designated as Shiga toxin 1 (*stx1*) and Shiga toxin 2 (*stx2*) [17] and our recent study revealed that *stx2* expression was associated with host immune gene expression and potential STEC colonization [18]. Although the distinctive fecal microbial communities has been reported in super-shedder (cattle shed $>10^4$ STEC in feces per gram, SS) compared to non-shedders [19], little knowledge is derived from *stx2* in STEC and its relationships with RAJ microbiota and microbial interactions. We speculated that microbial interactions together with the diversity and composition of RAJ microbiota are associated with *stx2* expression and STEC colonization in cattle. Hence, this study aimed to assess the rectal microbial communities and interactions in response to *stx2* expression in STEC at the RAJ, and the role of microbiota divergent in abundance among microbial interactions using the random matrix theory (RMT)- based method [20] and within-/among-module connectivity [21]. We aimed to identify keystone taxa and low abundant taxa contributing to microbial interaction networks and structural stability for better understanding the role of rectal microbiota in *stx2* expression and potential STEC colonization in beef cattle.

2. Materials and methods

2.1. Animal study and sample collection

The animal trial followed the Canadian Council of Animal Care guidelines and was confirmed by the Animal Care and Use Committee, University of Alberta with Animal Care Committee protocol number AUP00000882. The animal trial and identification of *stx2* gene abundance and expression were described in Pan et al. [18]. Briefly, ten cm^2 recto-anal junction (RAJ) tissue and 10 mL rectal contents were collected from a total of 143 feedlot cattle (585.84 ± 64.99 kg) within 30 min after slaughter at a federally approved abattoir.

DNA was extracted from 0.1 g powdered tissue using repeated bead beating and a column (RBBC) method [22], purified using the QIAmp Stool Mini Kit (Qiagen, Germany) and assessed based on absorbance at 260 and 280 nm using ND-1000 spectrophotometer (NanoDrop Technologies, Wilmington, USA). RNA was isolated from 0.1 g powered tissue using trizol reagent (Invitrogen Corporation, Carlsbad, CA, USA) method followed by manufacturer's protocols and assessed using Agilent 2200 TapeStation (Agilent Technologies, Santa Clara, CA, USA) and Qubit 3.0 Fluorometer (Invitrogen, USA). Tissue extracted DNA was subjected to detection of *stx2* gene abundance using quantitative PCR (qPCR) with primers 5′-ACTCTGACACCATCCTCT-3′ and 5′-CACTGTCTGAAACTGCTC-3′ [23]. Tissue extracted RNA was subjected to the identification of *stx2* transcript using reverse transcription real-time quantitative PCR (RT-qPCR) with the aforementioned primers [23]. Both PCR and RT-qPCR were conducted in triplicates for each sample and followed the same thermal program on a StepOnePlus™ Real-Time PCR System (Applied Biosystems, Foster City, CA, USA): one cycle at 95 °C for 20 s followed by 40 cycles of 3 s at 95 °C, 30 s at 60 °C. Twelve rectal digesta samples collected from steers whose mucosal samples were confirmed to possess *stx2* gene without expression (defined as Stx2− group) in the bacteria, and those with *stx2* and were expressed (defined as Stx2+ group, n = 6) in STEC were selected with minimized differences in body weight and age at slaughter between two groups based on one-way ANOVA ($P_{body\ weight}$ = 0.07, $P_{slaughter\ age}$ = 0.30, Table S1).

2.2. Amplicon sequencing and microbial community analysis

Total genomic DNA was extracted from frozen rectal digesta samples using the RBBC method [21], purified using the QIAmp Stool Mini Kit (Qiagen, Germany) following the manufacturer's protocols. The concentration and quality of DNA were further determined using the NanoDrop 2000 Spectrophotometer (Thermo Fisher Scientific, USA).

To generate the rectum bacterial compositional profiles, the bacterial V1-V3 region of the 16S rRNA gene was amplified using bacterial primers Bac9F (5′-GAGTTTGATCMTGGCTCAG-3′) and Ba515Rmod1 (5′-CCGCGGCKGCTGGCAC-3′) [20]. The PCR amplification products were verified using agarose gel (2%) electrophoresis. Two-step PCR was performed for PCR amplicon generation and barcoding. In detail, the PCR was conducted with the following thermal program of initial denaturation at 94 °C for 2 mins, followed by 33 cycles of 94 °C for 30 s, annealing at 58 °C for 30 s, elongation at 72 °C for 30 s, and at last a final elongation at 72 °C for 7 mins. Furthermore, the second PCR was performed using amplicons produced in the first step for barcoding with the following program: initial denaturation at 95 °C for 10 mins, followed by 15 cycles of 95 °C for 30 s, 60 °C for 30 s, 72 °C for 60 s, and a final elongation at 72 °C for 3 mins.

All amplicon libraries were sequenced using an Illumina MiSeq pair-end 300 bp platform at Centre d'expertise et de services Génome Québec (Quebec, Canada). The raw sequence data were assigned to each sample according to the corresponding barcode and were processed using QIIME2 (Version 2019.10) [24]. Quality control, denoising, removal of chimeric sequences, and generation of amplicon sequencing variants (ASVs) were performed using the QIIME2 plugin DADA2 [25]. Taxonomic classification was performed in QIIME2 using a taxonomic classifier with the SILVA database (version 132) as the reference. The Good's coverage index was used to evaluate the adequacy of sequencing depth to generate bacterial profiles in each sample. For diversity analyses, alpha diversity was estimated using Shannon (evenness) and Chao1 (richness) indices. Beta diversity was evaluated based on Weighted Unifrac distance using phylogenetic distances across identified taxa in a phylogenetic tree and the abundance of each feature to determine the similarity between Stx2− vs. Stx2+ groups. All diversity metrics were calculated using scripts implemented in QIIME2. The visualization of alpha- and beta- diversity was performed using the ggplot2 package in R. Differentially abundant (DA) genera (Absolute $\log_2$ fold change > 1 and false discovery rate <0.05) between Stx2− vs. Stx2+ groups were identified using the DESeq2 package in R. The cut-off of DA genera and group-specific taxa is a relative abundance >0.1% and presence in at least two out of six animals in each group.

2.3. Construction of microbial co-occurrence networks

The random matrix theory (RMT)-based method [8] was employed to construct the microbial co-occurrence network to identify microbial interactions using molecular ecological network analysis (MENA) (http://ieg4.rccc.ou.edu/mena) [8]. Briefly, the absolute abundance of microbial genera data was uploaded. The absolute abundance microbial genera dataset was appropriately standardized and the pairwise Pearson correlation suggested by the author's manual was employed to generate correlation coefficients and a similarity matrix firstly [8]. The similarity matrix was subsequently transformed into an adjacency matrix by applying the automatic generated threshold to the correlation values based on the RMT approach [8]. In this study, a connection stands for a strong (Pearson's r > 0.85) and significant (P < 0.01) correlation. The visualization of the co-occurrence network was performed using gephi (0.9.2).

2.4. Characterization of topological properties of co-occurrence networks

The modularity of each network was estimated using MENA along with the evaluation of other topological properties, including the clustering coefficient [26,27], average path length [28], graph density [29], and average degree [28]. Random networks and power-law distribution assessments were generated to evaluate whether empirical networks were prone to error and to identify microbiota interactions that were due to non-random patterns that represent the empirical structure of microbial communities [30,31]. Random networks were constructed based on the Maslov-Sneppen method [31] using MENA, which kept numbers of nodes (microbial taxa) and edges (connections) unchanged, but rewired positions of all links in the network.

From the network modularity perspective, taxa could be classified into network hubs, module hubs, connectors that represent generalists in the community, and peripherals that represent specialists in the community [32]. Generalists refer to taxa that are highly connected with others both within and among modules (network hubs), within a module (module hubs), and among different modules within a network (connectors). Specialists represent peripheral taxa that interact less with other taxa (including a node that is only connected within a module or at least 60% links within the module) [32]. Within-module connectivity (Zi) and among-module connectivity (Pi) were computed based on the following algorithm [32]:

$$Z_i = \frac{k_i - \overline{k}_{Si}}{\sigma_{ksi}}$$

where k_i is the number of links of node i to other nodes in its module s_i, $\overline{k}_{Si}$ is the average of k across all nodes in s_i, σ_{ksi} represents the standard deviation of k in s_i. Hence, Zi (within-module connectivity) characterizes to what extent node i is connected to others in its module.

$$P_i = 1 - \sum_{s=1}^{N_M} \left(\frac{k_{is}}{k_i}\right)^2$$

where k_{is} is the number of links of nodes i to nodes in module s, k_i is the total degree of node i within a network. Therefore, Pi (among-module connectivity) of a node stands for evenly distribution of links among all modules if its value is close to 1, and 0 if all its links are within its own module.

Zi and Pi were characterized using MENA with the classification as follows: network hubs (Zi > 2.5; Pi > 0.62), module hubs (Zi > 2.5; Pi < 0.62), connectors (Zi < 2.5; Pi > 0.62); peripherals (Zi < 2.5; Pi < 0.62) [21]. The thresholds for classifying nodes into aforementioned four roles in the network were determined by both heuristic determinations and the concept of 'basin of attraction' [21]. Briefly, Zi and Pi were both computed for each node in the network, and density plots were adopted to visualize the gradient of the value of Zi and Pi that can 'flow' to the local minimum (termed as 'basin of attraction'). In other words, the region of the space that 'flow' toward a certain minimum value is therefore regarded as the optimal threshold for Zi and Pi being 2.5 and 0.62, respectively [21].

Network stability is a critical component that tests if a network is resilient to perturbations sourced from external factors other than interactions [33,34]. Here, natural connectivity [35] was introduced to describe network stability differences in response to the *stx2* expression in STEC. The estimation of natural connectivity was based on the following algorithm:

$$\mathrm{ave}(\lambda) = \ln\left(\frac{1}{N}\sum_{i=1}^{N} e^{\lambda_i}\right)$$

where $\mathrm{ave}(\lambda)$ is the natural connectivity, N is the number of nodes in the network, λ_i is the eigenvalue of the adjacency matrix. A total of 137 nodes representing 80% of total nodes were randomly removed from the adjacency matrix and λ_i and $\mathrm{ave}(\lambda)$ were recalculated after each removal. The visualization of the natural connectivity was performed using the ggplot2 package in R.

The identification of potential hub microbial taxa in the network was validated using Lasso regression in R package 'glmnet'. Twelve samples were regarded as the training data with 9 samples (6 Stx2+; 3 Stx2−) as the external test data. The accuracy rate (the number of samples recognized correctly / total number of samples) was estimated to determine the model classification performance.

2.5. Data availability

All the sequencing data used in the current study has been submitted to NCBI Sequence Read Archive (SRA) under the accession numbers from SRR14769039 to SRR14769050 (BioProject ID PRJNA736180).

3. Results

3.1. Taxonomic assessment of the RAJ content-associated microbiota

A total of 179,917 filtered pair-end reads were generated with 14,993 ± 437 (mean ± SE) sequences per sample, and a total of 2,798 amplicon sequence variants (ASVs) were identified ranging from 174 to 275 (Table S2). The Good's coverage was >99.9% for all samples, indicating adequate sequencing depth.

From all samples, >99% of reads were classified into 13 phyla, with Firmicutes (72.7 ± 2.0%) and Bacteroidetes (24.6 ± 1.9%) being the most predominant phyla (relative abundance >10%, Additional file 1). At the family level, 59 families were identified with 7 unclassified and 52 classified (Additional file 1), of which *Ruminococcaceae* (47.2 ± 1.5%), *Lachnospiraceae* (9.2 ± 1.2%), and *Prevotellaceae* (8.8 ± 1.1%) were the most predominant families. At the genus level, 154 taxa were identified (Additional file 1, 20 unclassified; 134 classified), of which *Ruminococcaceae* UCG-005 (23.1 ± 2.1%) and *coprostanoligenes* group (9.1 ± 0.7%) from *Ruminococcaceae* family and *Christensenellaceae* R-7 group (7.3 ± 0.7%) from *Christensenellaceae* family were the most abundant genera. The most frequently detected genera (average relative abundance >0.5%, Additional file 1) belonged to Firmicutes (19 out of 27, 4 unclassified, 15 classified) and Bacteroidetes (8 out of 27, 1 unclassified, 8 classified), respectively.

There were 52 to 75 genera identified from each sample with 15 core genera shared by all 12 samples (Fig. 1A, Table S4). Specifically, 30.7% (4 out of 13 phyla, Firmicutes, Bacteroidetes, Actinobacteria, Proteobacteria), 18.6% (11 out of 59 families, 6 out of 11 belonged to Firmicutes; 5 out of 11 belonged to Bacteroidetes; Additional file 1) and 9.7% (15 out of 154 genera, 9 out of 15 belonged to Firmicutes; 6 out of 15 genera belonged to Bacteroidetes; Fig. 1A, Table S4,) were present in all samples. In addition, twenty-four genera were Stx2− specific and 13 genera were Stx2+ specific with 66 genera shared by both groups (Fig. 1B). Genera belonging to Firmicutes were the most predominant taxa in Stx2− (10 out of 24) and Stx2+ (4 out of 13) groups (Table S5).

3.2. Comparable diversity and composition of RAJ content-associated microbiota between Stx2− and Stx2+ groups

Neither Shannon nor Chao1 indices differed (Kruskal Wallis test, P > 0.05, Fig. 2A) between the bacterial communities from Stx2− and Stx2+ groups. Further comparison of the similarity of microbial communities between the two groups using ANOSIM (Analysis of similarities) revealed no clustering patterns (P = 0.52, Fig. 2B) at the phylum (P > 0.5, Fig. 3), family, or genus

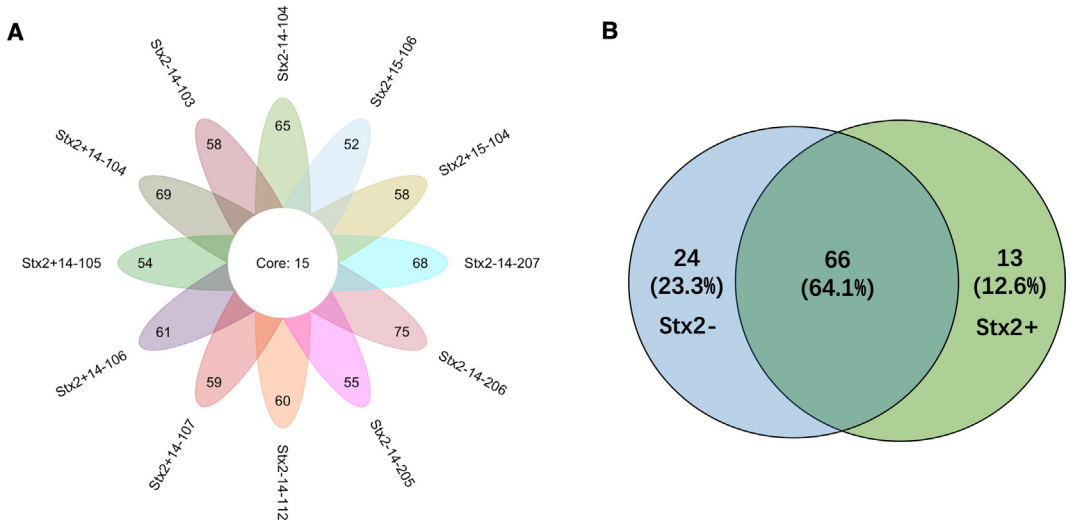

Fig. 1. Shared and specific genera between Stx2− and Stx2+ groups. A. The flower plot was used for visualization of the number of core genera shared by each sample (in the center) and the number of specific genera found in each sample (in the petals). B. Genera detected in Stx2+ and Stx2− group. Detected genera, total relative abundance of 0.1% within at least two samples in each group.

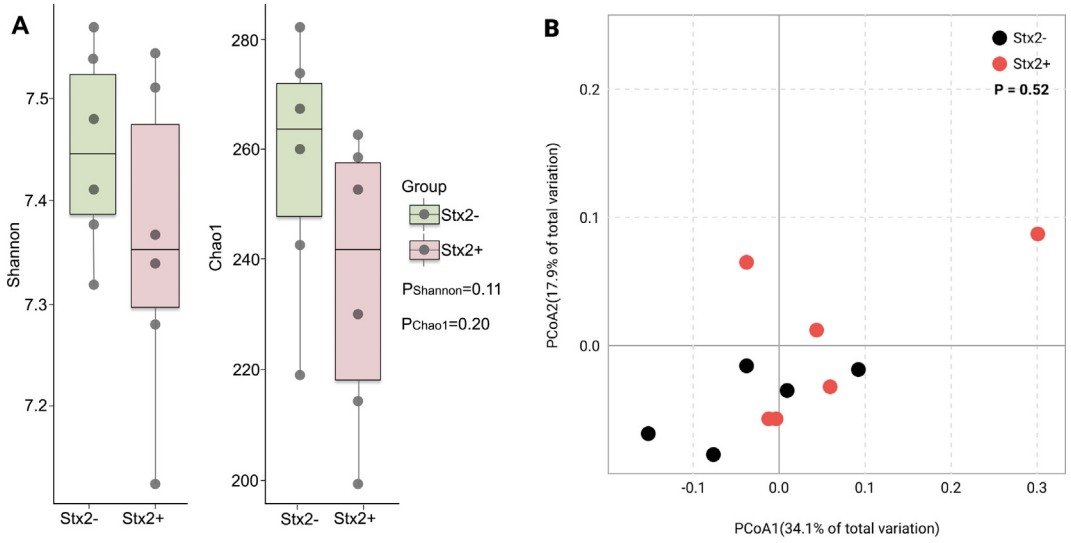

Fig. 2. Comparison of diversity metrics between Stx2− and Stx2+ groups. A. Shannon and Chao1 indices were used to estimate the evenness and richness between Stx2− and Stx2+ groups, respectively. The horizontal bars within boxes represent medians. The tops and bottoms of boxes represent the 75th and 25th percentiles, respectively. The upper and lower whiskers extend to data no >1.5× the interquartile range from the upper edge and lower edge of the box, respectively. The Kruskal-Wallis test was used to determine whether indices between the two groups were significant. ($P \leq 0.05$). B. Principal coordinate analysis (PCoA) was used for visualization of Weighted Unifrac distance. The PERMANOVA was used to test for the similarity of clustering patterns between Stx2− and Stx2+ groups. Differences were considered significant at $P \leq 0.05$.

(Both P > 0.1) levels. No differentially abundant taxa at the phylum, family, or genus level were identified between Stx2− and Stx2+ groups.

3.3. General co-occurrence patterns in each co-occurrence network

The non-random co-occurrence patterns were observed based on the significant power-law distribution in each group (R^2_{Stx2+} = 0.98, P < 0.05; R^2_{Stx2-} = 0.97, P < 0.01) as well as the greater value of structural properties in the empirical as compared to the random networks (Table 1). Hence, non-random empirical co-occurrence networks were established to uncover real-world microbial interactions. The empirical network consisted of 86 nodes (genera) with 322 edges (a mean of 7.49 edges per node) for Stx2− (Table 1, Fig. 4A), and 77 nodes with 243 edges for Stx2+ (Table 1, Fig. 4B). The average network distance between all paired nodes (average path length, APL) was 2.84 edges with a diameter (longest distance) of 8 edges in the Stx2− network and 2.86 edges with a diameter of 7 edges in the Stx2+ network, respectively (Table 1). The clustering coefficient (the degree to which nodes tend to cluster together) was 0.32 for the Stx2− network and 0.33 for the Stx2+ network, respectively (Table 1). The modularity index was 0.44 for the Stx2− network and 0.46 for the Stx2+ network (values >0.4 suggest that the network has a modular structure [36]) (Table 1).

3.4. Identification of keystone taxa and their associations with different co-occurrence patterns

High modularity was observed for both networks with 7 and 6 observed modules in the Stx2− and Stx2+ co-occurrence networks, respectively (Fig. 4A, B) with no network hubs being identified. More than 80% of nodes (Stx2−: 74 out of 86, 86.0%; Stx2+: 62 out of 77, 80.6%) with an abundance >0.2% were classified as

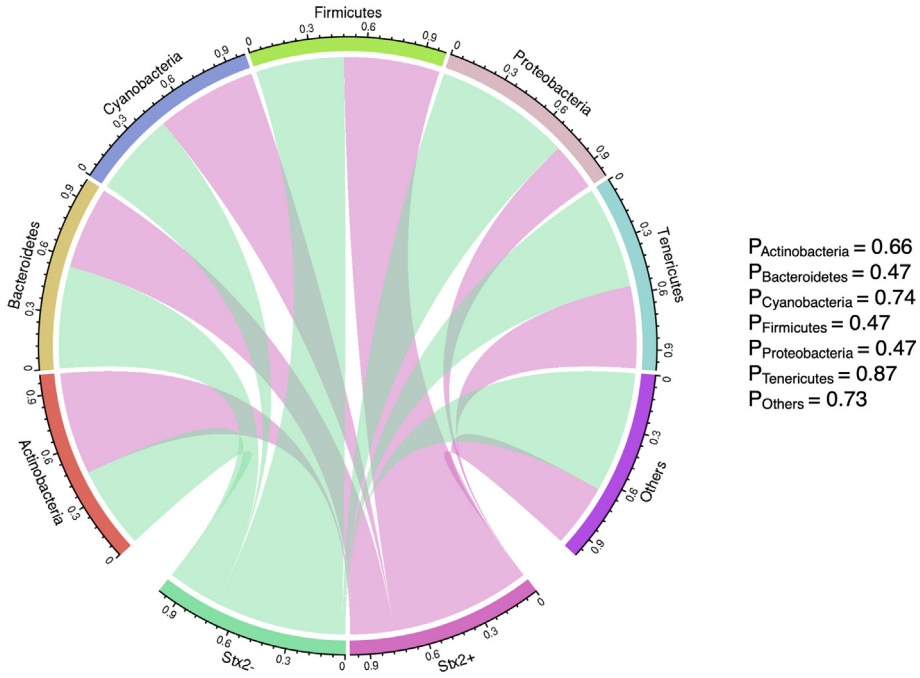

Fig. 3. Comparison of average relative abundance at the phylum level between Stx2− and Stx2+ groups. Circos plots were used for visualization of average relative abundance at the phylum level between Stx2− and Stx2+ groups. Phyla in each group with a total relative abundance of >0.1% in at least three samples were included. The Kruskal-Willas test was used to determine the average relative abundance of phyla was comparable (P > 0.05) between Stx2− and Stx2+ groups. P-values were false discovery rate (FDR, q = 0.05) adjusted.

Table 1
Topological properties of empirical and random network between Stx2− and Stx2+ groups.

	Empirical network		Random network	
Group	Stx2−	Stx2+	Stx2−	Stx2+
Nodes	86	77	86	77
Edges	322	243	322	243
Modularity (MD)	0.44	0.46	0.29 (±0.011)	0.31 (±0.012)
Clustering coefficient (CC)	0.32	0.30	0.12 (±0.014)	0.12 (±0.016)
Average path length (APL)	2.84	2.86	2.47 (±0.030)	2.58 (±0.033)
Graph density (GD)	0.088	0.083	0.09	0.08
Average degree (AD)	7.49	6.31	7.49	6.31

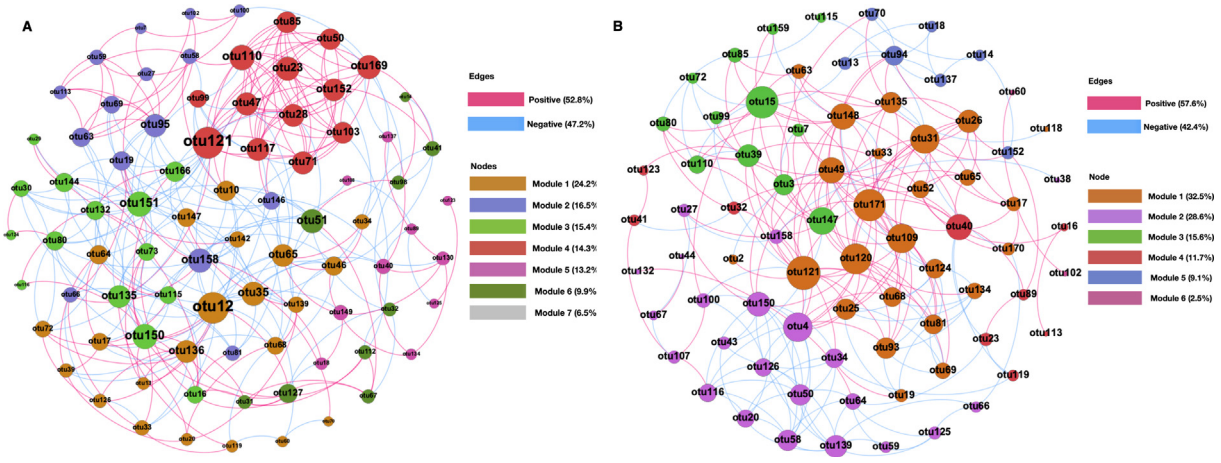

Fig. 4. Co-occurrence networks of bacterial genera in (A) Stx2− and (B) Stx2+ groups. The size of each node is proportional to the number of connections (that is, degree); the color of connections between two nodes represents a positive (red) or a negative correlation (blue). Each module is presented as a specific color. (For interpretation of the references to color in this figure legend, the reader is referred to the web version of this article.)

peripherals (Fig. 5A). Only 14% (connectors: 11 out of 86; module hubs: 1 out of 86; Stx2− group) and 19.4% (connectors: 14 out of 77; module hubs: 1 out of 77; Stx2+ group) of taxa from Stx2− and Stx2+, respectively, were designated as specialists (Fig. 5A). Specifically, >85% (23 out of 27) of connectors had a lower abundance (<0.2%) with a high Pi value (0.62 ∼ 0.77) (Fig. 5B).

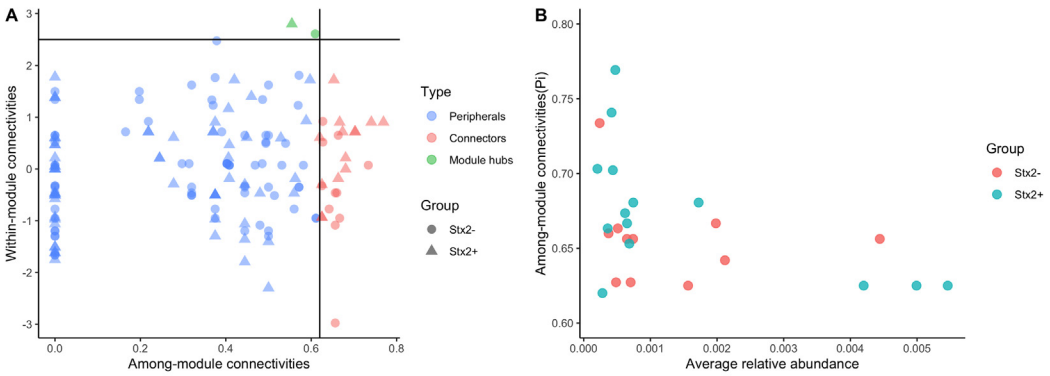

Fig. 5. Distribution and average relative abundance of genera based on their network roles. A. Distribution of bacterial genera based on their network roles. Nodes in the network were classified as peripherals, modular hubs, or connectors. No network hubs were identified in networks from both groups. B. Average relative abundance of connectors.

Furthermore, generalists formed differential clustering patterns between Stx2− and Stx2+ networks. Generalists were evenly distributed across identified ecological clusters in the Stx2− network. Four out of fourteen generalists belonged to module 3, whereas other generalists were in module 1 (3 out of 11), module 2 (2 out of 11), module 4 (1 out of 11), module 5 (1 out of 11) and module 6 (1 out of 11). However, in the Stx2+ network generalists were not evenly distributed with 7, 4, 3, and 1 out of 14 generalists belonging to modules 1, 3, 2, and 4, respectively.

Moreover, decreased stability of the network was evidenced by reduced natural connectivity in the Stx2+ network in comparison to the Stx2− network (Fig. 6). The natural connectivity that supported network stability in each group gradually decreased with the increasing number of removed nodes, while natural connectivity in the Stx2+ network always being lower than that in the Stx2− network regardless of the numbers of nodes removed from each network (Fig. 6).

3.5. Group-specific taxa as keystone taxa in microbial interactions

More than 50% of the group-specific genera (8 out of 12 in Stx2−; 6 out of 12 in Stx2+, Table 2) belonged to generalists with a lower abundance (relative abundance <0.2%). Group-specific generalists in the Stx2− network included: *Parvibacter*, *Candidatus saccharimonas*, *Acetitomaculum,* as well as unknown genera within the Bacteroidetes, Proteobacteria, Tenericutes, Cyanobacteria, and the *Veillonellaceae*. Besides, among generalists in the Stx2+ network, *Prevotellaceae* Ga6A1 group, *Flexilinea, Ruminiclostridium* 9, *Ruminococcus* 1, *Acetobacter*, and *Streptomyces* were group-specific genera in microbial communities in the Stx2+ group. All the core microbes shared by two groups (Fig. 3B) were regarded as specialists that were poorly connected with other taxa within networks.

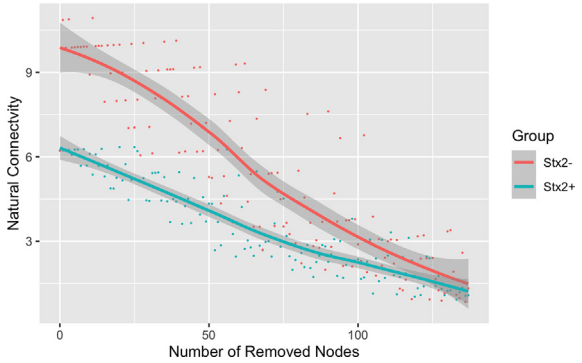

Fig. 6. The natural connectivity representing the network stability of co-occurrence networks in both Stx2− and Stx2+ groups.

Table 2
Stx2− and Stx2+ generalists at genus level and their belonged bacterial phyla.

Phylum	Genus	Group-specific
Stx2− group		
Actinobacteria	*Parvibacter*	Stx2− specific
Bacteroidetes	f_*Bacteroidales* RF16 group	
	f_ *Prevotellaceae*	Stx2− specific
Cyanobacteria	o_ *Gastranaerophilales*	Stx2− specific
Firmicutes	f_ *Veillonellaceae*	Stx2− specific
	Acetitomaculum	Stx2− specific
	f_ *Veillonellaceae*	
Patescibacteria	*Candidatus saccharimonas*	Stx2− specific
Planctomycetes	p-1088-a5 gut group	
Proteobacteria	*Parasutterella*	
	o_ *Rhodospirillales*	Stx2− specific
Tenericutes	o_ *Izimaplasmatales*	Stx2− specific
Stx2+ group		
Actinobacteria	*Saccharopolyspora rectivirgula*	
	Streptomyces	Stx2+ specific
Bacteroidetes	*Prevotellaceae* Ga6A1 group	Stx2+ specific
	Prevotellaceae UCG-001	
	Parabacteroides	
Chloroflexi	*Flexilinea*	Stx2+ specific
Firmicutes	*Oscillibacter*	
	Ruminiclostridium 9	Stx2+ specific
	Ruminococcus 1	Stx2+ specific
	f_ *Erysipelotrichaceae*	
	Cellulosilyticum	
Planctomycetes	p-1088-a5 gut group	
Proteobacteria	*Acetobacter*	Stx2+ specific
	Parasutterella	

4. Discussion

This study assessed microbial interactions in response to *stx2* expression in STEC at RAJ in beef steers, shedding light on microbial mechanisms regulating STEC colonization as well as providing novel approaches to understanding differences in microbial communities. The compositional profiles of microbial communities identified in our study were comparable to those identified from the rectum content of dairy cattle [37], and fecal microbiota of beef cattle [19,38] with the most dominant phyla being Firmicutes and Bacteroidetes with an accumulative relative abundance of up to 94.1%, 89.5%, and 80.6%, respectively. The proportion of three main families (*Ruminococcaceae* (47.2 ± 1.5%), *Lachnospiraceae* (9.2 ± 1.2%), and *Prevotellaceae* (8.8 ± 1.1%)) were also similar to

the bacterial taxa identified in a study where cattle were shedding >10^4 cfu/g of *E. coli* O157 in that 31.8%, 10.5%, 9.0% of total reads from fecal microbiota were assigned to *Ruminococcaceae, Prevotellaceae,* and *Lachnospiraceae,* respectively [19]. Although all cattle were raised under the same high-grain diet and management conditions and were similar in age and body weight, individual variations of microbial communities were still observed including the relative abundance of each microbial community and the proportion of predominant taxa shared by each microbial community. Variation in the microbial fecal profile of individual cattle has been previously reported [19], a finding that has been attributed to differences in age, weight, and diet. As these variables were relatively consistent in our study, other host factors along with microbial crosstalk within the microbiota might be the main drivers for the individualized microbial composition.

Despite highly similar microbial profiles including comparable alpha and beta diversity between Stx2− and Stx2+ groups, microbial interactions within the microbiota varied. Microbes can interact with each other for the purpose of co-evolution [39] leading to adaptation and specialization [39] of certain microbial taxa, which promote future alterations in the microbial community. To date, the widely used approaches to study the microbial interactions is based on network construction mainly using correlation-based (Pearson's and Spearman correlation coefficient) and maximal information coefficient (MIC) methods that have proven to be less useful in inferring microbial ecological networks assessed by area under the precision-recall curves (AUPR) [3]. These metrics (*i.e.,* correlation-based approaches, MIC) are less applicable to microbial compositional data as the assumption of independent variables can be satisfied, leading to the generation of spurious correlations [3,40], and therefore are less powerful for inferring real microbial interactions. To overcome such limitations in this study, similarity matrix was first established using Pearson's correlations and then the RMT-based approach was employed to determine the reference point which enables automatic threshold selection and minimizes noise. The RMT-based approach was established based on two universal roles of random matrix theory: the distribution of two nearest eigenvalues follows Gaussian orthogonal ensemble (GOE) statistics correlations exist (a true correlation will follow GOE distribution in RMT theory), while it follows Poisson distribution if there is no correlation [41]. Particularly the transition between GOE and Poisson distribution serves as the reference point to distinguish non-random relationships (that is true correlations) in the data matrix from background noise [41]. In other words, a correlation refers to the GOE distribution while non-correlation represents the Poisson distribution and the transition point from GOE to Poisson distribution is the reference point for the automatic generated threshold used for the construction of the microbial network and the identification of meaningful correlations from the noise (*i.e.* certain correlations might not follow GOE and therefore could be noise or spurious correlations). Hence, compared to studies that only adopt correlations (Pearson's and Spearman correlation coefficient) for constructing microbial networks, the RMT-based approach is more effective at identifying true interactions within the response networks to *stx2* expression.

Comparison of random and empirical networks based on topological properties, confirmed constructed networks were effective for investigating interactions between *stx2* expression and microbial communities. Particularly, modules (clusters) were powerful topological features to reflect network differences, referring to the fundamental units whose constituent elements (nodes) are functionally similar in terms of specific chemical, and biological processes [42]. Previous explorations in soil-microbial interactions revealed that clusters in the network have specific and different functions that enable microbes to respond to different soil conditions [43,44]. For instance, three major modules with diverse functions (electron-transfer, biogeochemical C- and N- cycles, organic contaminant degradation) were characterized for microbial communities from soil contaminated with oil [44], Clusters were shown to be crucial components of microbial communities in the network and necessary to develop an understanding of modularity in networks and microbial interactions. The Stx2− and Stx2+ groups formed comparable numbers of clusters while clusters in each group included different taxa, suggesting functions of clusters in each group differed in their interactions in response to *stx2* expression in STEC at RAJ. Regardless, the highly connected genera among densely connected clusters of nodes (that is, modules) were observed in both Stx2− and Stx2+ groups resulting in the formation of 'small world' topologies, indicative of empirical networks that are more clustered than random networks.

Identifications of generalists also furthered the understanding of microbial community structure and differential microbial interactions, which play an empirical rather than theoretical role among microbial interactions. Particularly, identified generalists in our study are group-specific taxa, which are with low relative abundance but might play unique roles such as regulating microbial interactions within each network through nutritional supplementation or competition. *E. coli* O157:H7 can utilize ethanolamine as the free nitrogen source in the bovine small intestine, thus the presence or absence of ethanolamine utilizing bacteria could be a contributing factor to diverse microbial communities [19,45]. In our study, *Streptomyces* identified as Stx2+ specific genera were capable of metabolizing ethanolamine [46], which might generate a niche for the survival of *stx2* expressed bacteria. However, not all group-specific generalists in microbial communities play a role in nutrient supplementation for STEC. For instance, *Acetobacter* (a group-specific generalist from the Stx2+ group) is capable of converting ethanol to acetic acid which can inhibit STEC [47]. A similar case is also observed in Stx2− group that *Acetitomaculum* (a group-specific generalist from Stx2− group), an acetogenic bacteria [48], may also suppress STEC. It is noticeable that >85% (23 out of 27) generalists were low abundant taxa with an average abundance <0.2%, highlighting the irreplaceable role of rare abundant taxa among microbial interactions. For instance, rare *Methanotrophs* (*i.e. Methylocaldum*) acting as 'primary producers' in methane-driven food webs [49], rare symbionts (*i.e. Symbiodinium*) increase coral-algal assembly stability with environmental alterations [50]. Hence, these results raise the possibility that less abundant group-specific generalists contribute to the differential degradation of organic matter and play a practical role in microbial interactions by mediating nutrient availability in a manner that may have positive or negative effects on STEC colonization. The lack of well-defined approaches for determining keystone taxa from networks embedded our understanding of microbial interactions. Previous studies adopted global topological properties (*i.e.* betweenness centrality) for inferring keystone taxa [51], which neglects the fact that networks tend to be modular. Identification of generalists (or keystone taxa) following the concept of among/within- module connectivity provides the added advantage for further understanding of microbial interactions. Thus, the approach in our study of using the concept of modularity to compute the role of each node is more representative of network modularity and the role of each node with/among the overall structure.

As a supportive approach, lasso regression revealed group-specific microbes contributed to the mucosa-associated *stx2* expression. Among the 7 selected genera based on lasso regression, 2 out of 7 were core and 3 out of 7 were group-specific genera (Table S6). However, all of the core microbes were identified as peripherals that were poorly connected with other taxa and were not expected to affect the robustness of the network [52]. Compared to studies that emphasize the value of core microbiota in the maintenance of microbial communities, group-specific genera

exhibiting diverse functions could potentially interact with the host and Stx2-carrying/Stx2-expressed bacteria, leading to the establishment of a different co-occurrence network. Hence, our study highlights the valuable role of group-specific taxa in the microbial co-occurrence network which advances the understanding of microbial interactions in terms of *stx2* expression and potential STEC colonization. It is noticeable that the identified microbial networks should be validated in the future. In addition to the mathematical algorithm that reduces spurious correlations, adding stable isotope probes in the DNA-derived microbial community and analyzing heavy-isotope enriched DNA could be alternative approach, which could differentiate inactive microbial interactions from ecological meaningful microbial crosstalk left [53,54]. For instance, a DNA-based stable isotope probing approach using [^{13}C]CH_4 has been employed to identify real microbial interactions by co-occurrence analysis in ombrotrophic peatlands [53]. However, using heavy isotope probes to examine true microbial interactions within the dense microbial communities of the gut needs further evaluation.

5. Conclusions

Overall, our results revealed comparable diversity and composition of RAJ microbiota were observed between Stx2− and Stx2+ animals with >60% genera recognized as members of the core microbiome. However, RMT-based network analysis revealed varried microbial interactions, keystone taxa, and stability of microbial communities in response to *stx2* expression. Group-specific taxa play an unusual role in the network which might drive microbiota-*stx2* interactions. This study also constitutes an in-depth understanding of host-STEC interactions and highlights the possibility of altering the gut environment to mitigate *stx2* expression through modifying the gut microbiota. However, future validations using a larger sample size are needed to verify the proposed methods for deciphering microbial community differences as well as the principles of microbe coexistence that determine microbial interactions. Regardless, our findings highlight the critical role of group-specific genera among microbial interactions and shed light on using an integrated approach that integrates group-specific genera with network analysis to identify and characterize differences in microbial communities with comparable microbial profiles.

Author statement

ZP involved in concept development, performed data analysis and manuscript writing. YC contributed to sample collection, lab work and data generation. MZ involved in microbiota data analysis and manuscript revision. TAM involved in data interpretation and manuscript revision. LLG involved in the concept of the study, data analysis and manuscript writing.

Declaration of Competing Interest

The authors declare that they have no known competing financial interests or personal relationships that could have appeared to influence the work reported in this paper.

Acknowledgement

This study is supported by Beef Cattle Research Council (BCRC, FOS.07.17) and NSERC Discovery grant, and the authors thank staffs at Lacombe Research Centre, Drs, H. Sun, F. Li as well as J. H. Liu, A. Bulumulla for their assistance in sample collection.

Appendix A. Supplementary data

Supplementary data to this article can be found online at https://doi.org/10.1016/j.csbj.2021.10.035.

References

[1] Le Chatelier E, Nielsen T, Qin J, Prifti E, Hildebrand F, Falony G, et al. Richness of human gut microbiome correlates with metabolic markers. Nature 2013;500 (7464):541–6. https://doi.org/10.1038/nature12506.
[2] Derakhshani H, Plaizier JC, Buck JD, Barkema HW, Khafipour E. Composition and co-occurrence patterns of the microbiota of different niches of the bovine mammary gland: potential associations with mastitis susceptibility, udder inflammation, and teat-end hyperkeratosis. Animal Microbiome 2020;2:11. https://doi.org/10.1186/s42523-020-00028-6.
[3] Hirano H, Takemoto K. Difficulty in inferring microbial community structure based on co-occurrence network approaches. BMC Bioinf 2019;20:329. https://doi.org/10.1186/s12859-019-2915-1.
[4] Zhou J, Deng Y, Luo F, He Z, Tu Q, Zhi X, et al. Functional molecular ecological networks. Mbio 2010;1(4). https://doi.org/10.1128/mBio.00169-10.
[5] Guo W, Zhou Mi, Ma T, Bi S, Wang W, Zhang Y, et al. Survey of rumen microbiota of domestic grazing yak during different growth stages revealed novel maturation patterns of four key microbial groups and their dynamic interactions. Animal Microbiome 2020;2(1). https://doi.org/10.1186/s42523-020-00042-8.
[6] Zhang B, Horvath S. A general framework for weighted gene co-expression network analysis. Stat Appl Genet Mol 2005;4:Article17. https://doi.org/10.2202/1544-6115.1128.
[7] Xia Y. Chapter Eleven Correlation and association analyses in microbiome study integrating multiomics in health and disease. Prog Mol Biol Transl 2020;171:309–491. https://doi.org/10.1016/bs.pmbts.2020.04.003.
[8] Deng Y, Jiang YH, Yang Y, He Z, Luo F, Zhou J. Molecular ecological network analyses. BMC Bioinformatics 2012;13:113. https://doi.org/10.1186/1471-2105-13-113.
[9] Karmali MA, Petric M, Steele BT, Lim C. Sporadic cases of haemolytic-uraemic syndrome associated with faecal cytotoxin and cytotoxin-producing escherichia coli in stools. Lancet 1983;321(8325):619–20. https://doi.org/10.1016/S0140-6736(83)91795-6.
[10] Sheng H, Lim JY, Knecht HJ, Li J, Hovde CJ. Role of Escherichia coli O157:H7 virulence factors in colonization at the bovine terminal rectal mucosa. Infect Immun 2006;74(8):4685–93. https://doi.org/10.1128/IAI.00406-06.
[11] Donkersgoed JV, Berg J, Potter A, Hancock D, Besser T, Rice D, et al. Environmental sources and transmission of Escherichia coli O157 in feedlot cattle. Can Vet J La Revue Vétérinaire Can 2001;42:714–20.
[12] Munns KD, Selinger LB, Stanford K, Guan L, Callaway TR, McAllister TA. Perspectives on Super-Shedding of Escherichia coli O157:H7 by Cattle. Foodborne Pathog Dis 2015;12(2):89–103. https://doi.org/10.1089/fpd.2014.1829.
[13] Wang O, Liang G, McAllister TA, Plastow G, Stanford K, Selinger B, et al. Comparative transcriptomic analysis of rectal tissue from beef steers revealed reduced host immunity in Escherichia coli O157:H7 super-shedders. PLoS ONE 2016;11(3):e0151284. https://doi.org/10.1371/journal.pone.0151284.
[14] Wang O, McAllister TA, Plastow G, Stanford K, Selinger B, Guan LL. Host mechanisms involved in cattle Escherichia coli O157 shedding: a fundamental understanding for reducing foodborne pathogen in food animal production. Sci Rep-Uk 2017;7:7630. https://doi.org/10.1038/s41598-017-06737-4.
[15] Wang O, McAllister TA, Plastow G, Stanford K, Selinger B, Guan LL, et al. Interactions of the hindgut mucosa-associated microbiome with its host regulate shedding of Escherichia coli O157:H7 by cattle. Appl Environ Microb 2018;84(1). https://doi.org/10.1128/AEM.01738-17.
[16] Wang O, Zhou M, Chen Y, McAllister TA, Plastow G, Stanford K, et al. MicroRNAomes of cattle intestinal tissues revealed possible miRNA regulated mechanisms involved in Escherichia coli O157 fecal shedding. Front Cell Infect Mi 2021;11. https://doi.org/10.3389/fcimb.2021.634505.
[17] Fraser ME, Fujinaga M, Cherney MM, Melton-Celsa AR, Twiddy EM, O'Brien AD, et al. Structure of Shiga Toxin Type 2 (Stx2) from Escherichia coli O157:H7*. J Biol Chem 2004;279(26):27511–7. https://doi.org/10.1074/jbc.M401939200.
[18] Pan Z, Chen Y, McAllister TA, Gänzle M, Plastow G, Guan LL. Abundance and expression of shiga toxin genes in Escherichia coli at the recto-anal junction relates to host immune genes. Front Cell Infect Mi 2021;11:. https://doi.org/10.3389/fcimb.2021.633573633573.
[19] Xu Y, Dugat-Bony E, Zaheer R, Selinger L, Barbieri R, Munns K, et al. Escherichia coli O157:H7 super-shedder and non-shedder feedlot steers harbour distinct fecal bacterial communities. PLoS ONE 2014;9(5):e98115. https://doi.org/10.1371/journal.pone.0098115.
[20] Zhou J, Deng Y, Luo F, He Z, Yang Y, Relman D. Phylogenetic molecular ecological network of soil microbial communities in response to elevated CO2. Mbio 2011;2(4). https://doi.org/10.1128/mBio.00122-11.
[21] Yu Z, Morrison M. Improved extraction of PCR-quality community DNA from digesta and fecal samples. Biotechniques 2004;36(5):808–12. https://doi.org/10.2144/04365ST04.
[22] He Li, Simpson DJ, Gänzle MG. Detection of enterohaemorrhagic Escherichia coli in food by droplet digital PCR to detect simultaneous virulence factors in a

single genome. Food Microbiol 2020;90:103466. https://doi.org/10.1016/j.fm.2020.103466.
[23] E. Bolyen J.R. Rideout M.R. Dillon N.A. Bokulich C.C. Abnet G.A. Al-Ghalith et al. Author Correction: Reproducible, interactive, scalable and extensible microbiome data science using QIIME 2 Nat Biotechnol 37 9 2019 1091 1091 10.1038/s41587-019-0252-6
[24] Callahan BJ, McMurdie PJ, Rosen MJ, Han AW, Johnson AJA, Holmes SP. DADA2: High-resolution sample inference from Illumina amplicon data. Nat Methods 2016;13(7):581–3. https://doi.org/10.1038/nmeth.3869.
[25] Watts DJ, Strogatz SH. Collective dynamics of 'small-world' networks. Nature 1998;393(6684):440–2. https://doi.org/10.1038/30918.
[26] Ravasz E, Somera AL, Mongru DA, Oltvai ZN, Barabási A-L. Hierarchical organization of modularity in metabolic networks. Science 2002;297(5586):1551–5. https://doi.org/10.1126/science:1073374.
[27] Albert R, Barabási A-L. Statistical mechanics of complex networks. Rev Mod Phys 2002;74(1):47–97. https://doi.org/10.1103/RevModPhys.74.47.
[28] Wolfe AW. Social network analysis: methods and applications. Am Ethnol 1997;24:219–20. https://doi.org/10.1525/ae.1997.24.1.219.
[29] Horner-Devine MC, Silver JM, Leibold MA, Bohannan BJM, Colwell RK, Fuhrman JA, et al. A comparison of taxon co-occurrence patterns for macro- and microorganismS. Ecology 2007;88(6):1345–53. https://doi.org/10.1890/06-0286.
[30] Barberán A, Bates ST, Casamayor EO, Fierer N. Using network analysis to explore co-occurrence patterns in soil microbial communities. Isme J 2012;6(2):343–51. https://doi.org/10.1038/ismej.2011.119.
[31] Maslov S, Sneppen K. Specificity and stability in topology of protein networks. Arxiv 2002;296(5569):910–3. https://doi.org/10.1126/science:1065103.
[32] Guimerà R, Nunes Amaral LA. Functional cartography of complex metabolic networks. Nature 2005;433(7028):895–900. https://doi.org/10.1038/nature03288.
[33] Hicklin A. Network stability: opportunity or obstacles? Public Organization Rev 2004;4(2):121–33. https://doi.org/10.1023/B:PORJ.0000031625.78226.bc.
[34] Csermely P. Weak links, the universal key to the stability of networks and complex systems. Front Collect 2009:53–100. https://doi.org/10.1007/978-3-540-31157-7_3.
[35] Jun W, Barahona M, Yue-Jin T, Hong-Zhong D. Natural connectivity of complex networks. Chinese Phys Lett 2010;27(7):078902. https://doi.org/10.1088/0256-307X/27/7/078902.
[36] Newman MEJ. Modularity and community structure in networks. Proc National Acad Sci 2006;103(23):8577–82. https://doi.org/10.1073/pnas.0601602103.
[37] Mao S, Zhang M, Liu J, Zhu W. Characterising the bacterial microbiota across the gastrointestinal tracts of dairy cattle: membership and potential function. Sci Rep-Uk 2015;5:16116. https://doi.org/10.1038/srep16116.
[38] Shanks OC, Kelty CA, Archibeque S, Jenkins M, Newton RJ, McLellan SL, et al. Community structures of fecal bacteria in cattle from different animal feeding operations. Appl Environ Microb 2011;77(9):2992–3001. https://doi.org/10.1128/AEM.02988-10.
[39] Braga RM, Dourado MN, Araújo WL. Microbial interactions: ecology in a molecular perspective. Braz J Microbiol 2016;47:86–98. https://doi.org/10.1016/j.bjm.2016.10.005.
[40] Aitchison J. A new approach to null correlations of proportions. J Int Ass Math Geol 1981;13(2):175–89. https://doi.org/10.1007/BF01031393.
[41] Luo F, Yang Y, Zhong J, Gao H, Khan L, Thompson DK, et al. Constructing gene co-expression networks and predicting functions of unknown genes by random matrix theory. BMC Bioinf 2007;8(1). https://doi.org/10.1186/1471-2105-8-299.
[42] Lecca P, Re A. Detecting modules in biological networks by edge weight clustering and entropy significance. Front Genet 2015;6:265. https://doi.org/10.3389/fgene.2015.00265.
[43] Shi Yu, Delgado-Baquerizo M, Li Y, Yang Y, Zhu Y-G, Peñuelas J, et al. Abundance of kinless hubs within soil microbial networks are associated with high functional potential in agricultural ecosystems. Environ Int 2020;142:105869. https://doi.org/10.1016/j.envint.2020.105869.
[44] Jiao S, Liu Z, Lin Y, Yang J, Chen W, Wei G. Bacterial communities in oil contaminated soils: Biogeography and co-occurrence patterns. Soil Biology Biochem 2016;98:64–73. https://doi.org/10.1016/j.soilbio.2016.04.005.
[45] Bertin Y, Girardeau JP, Chaucheyras-Durand F, Lyan B, Pujos-Guillot E, Harel J, et al. Enterohaemorrhagic Escherichia coli gains a competitive advantage by using ethanolamine as a nitrogen source in the bovine intestinal content. Environ Microbiol 2011;13:365–77. https://doi.org/10.1111/j.1462-2920.2010.02334.x.
[46] Krysenko S, Matthews A, Okoniewski N, Kulik A, Girbas MG, Tsypik O, et al. Initial metabolic step of a novel ethanolamine utilization pathway and its regulation in streptomyces coelicolor M145. Mbio 2019;10. https://doi.org/10.1128/mbio.00326-19.
[47] Han K, Lim HC, Hong J. Acetic acid formation in escherichia coli fermentation. Biotechnol Bioeng 1992;39(6):663–71. https://doi.org/10.1002/bit.260390611.
[48] le Van TD, Robinson JA, Ralph J, Greening RC, Smolenski WJ, Leedle JAZ, et al. Assessment of reductive acetogenesis with indigenous ruminal bacterium populations and Acetitomaculum ruminis. Appl Environ Microb 1998;64(9):3429–36. https://doi.org/10.1128/AEM.64.9.3429-3436.1998.
[49] Lu L, Li X, Li Z, Chen Y, Sabio y García CA, Yang J, et al. Aerobic methanotrophs in an urban water cycle system: Community structure and network interaction pattern. Sci Total Environ 2021;772:145045. https://doi.org/10.1016/j.scitotenv.2021.145045.
[50] Ziegler M, Eguíluz VM, Duarte CM, Voolstra CR. Rare symbionts may contribute to the resilience of coral–algal assemblages. Isme J 2018;12(1):161–72. https://doi.org/10.1038/ismej.2017.151.
[51] Poudel R, Jumpponen A, Schlatter DC, Paulitz TC, Gardener BBM, Kinkel LL, et al. Microbiome networks: a systems framework for identifying candidate microbial assemblages for disease management. Phytopathology 2016;106(10):1083–96. https://doi.org/10.1094/PHYTO-02-16-0058-FI.
[52] Memmott J, Waser NM, Price MV. Tolerance of pollination networks to species extinctions. Proc Royal Soc Lond Ser B Biological Sci 2004;271(1557):2605–11. https://doi.org/10.1098/rspb.2004.2909.
[53] Kaupper T, Mendes LW, Harnisz M, Krause SMB, Horn MA, Ho A, et al. Recovery of methanotrophic activity is not reflected in the methane-driven interaction network after peat mining. Appl Environ Microb 2021;87(5). https://doi.org/10.1128/AEM.02355-20.
[54] Kaupper T, Mendes LW, Lee HJ, Mo Y, Poehlein A, Jia Z, et al. When the going gets tough: emergence of a complex methane-driven interaction network during recovery from desiccation-rewetting. Soil Biology Biochem 2021;153:108109. https://doi.org/10.1016/j.soilbio.2020.108109.